

available at www.sciencedirect.com

ScienceDirect

www.elsevier.com/locate/molonc

N-terminal targeting of androgen receptor variant enhances response of castration resistant prostate cancer to taxane chemotherapy

Sarah K. Martin^a, Carmen A. Banuelos^b, Marianne D. Sadar^b,
Natasha Kyprianou^{a,c,d,*}

^aDepartment of Molecular and Cellular Biochemistry, University of Kentucky College of Medicine, Lexington, KY, USA

^bDepartment of Genome Sciences Centre, BC Cancer Agency, Vancouver, BC, Canada

^cDepartment of Urology, University of Kentucky, Lexington, USA

^dMarkey Cancer Center, University of Kentucky, Lexington, KY, USA

ARTICLE INFO

Article history:

Received 5 August 2014

Received in revised form

3 October 2014

Accepted 29 October 2014

Available online 15 November 2014

Keywords:

Prostate cancer

Androgen signaling

Taxanes

Therapeutic resistance

Epithelial-mesenchymal transition

ABSTRACT

Taxane-based chemotherapy is an effective treatment for castration-resistant-prostate cancer (CRPC) via stabilization of microtubules. Previous studies identified that the inhibitory effect of microtubule-targeting chemotherapy on androgen receptor (AR) activity was conferred by interfering with AR intracellular trafficking. The N-terminal domain (NTD) of AR was identified as a tubulin-interacting domain that can be effectively targeted by the novel small molecule inhibitor, EPI. Taken together this evidence provided the rationale that targeting AR nuclear translocation and activity via a combination of an antagonist of the AR NTD and taxane-based chemotherapy may enhance the therapeutic response in CRPC. The present study investigated the anti-tumor efficacy of a combination of EPI with Docetaxel chemotherapy, in cell models of CRPC, harboring the AR splice variants in addition to the full length AR. Our findings demonstrate that there was no significant effect on the androgen-mediated nuclear transport of AR variants and AR transcriptional activity by Docetaxel. The therapeutic response to Docetaxel was enhanced by inhibition of the NTD of AR (by EPI) through cycling of epithelial-mesenchymal-transition (EMT) to mesenchymal-epithelial-transition (MET) among prostate cancer epithelial cells. These results support that transient “programming” of EMT by the AR NTD inhibitor, potentially drives the sensitivity of prostate tumors with differential distribution of AR variants to microtubule-targeting chemotherapy. This study is of major significance in dissecting mechanisms to overcome taxane resistance in advanced CRPC.

© 2014 Federation of European Biochemical Societies. Published by Elsevier B.V. All rights reserved.

Abbreviations: ADT, androgen deprivation therapy; AR, androgen receptor; AR-V, androgen receptor splice variant; CRPC, castration-resistant prostate cancer; DHT, dihydrotestosterone; EMT, epithelial mesenchymal transition; ERG, ETS-related gene; FOXO1, forkhead box O1; FZD4, Frizzled4; LBD, ligand-binding domain; LH, luteinizing hormone; LHRH, luteinizing hormone releasing hormone; NTD, N-terminal domain; PSA, prostate specific antigen; PTEN, phosphatase and tensin homolog; DMSO, dimethylsulfoxide; BrdU, bromodeoxyuridine; TUNEL, terminal deoxynucleotidyl transferase dUTP nick-end-labeling.

* Corresponding author. Department of Urology, University of Kentucky College of Medicine, 800 Rose Street, Lexington, KY 40536, USA. Tel.: +1 859 323 9812; fax: +1 859 323 6679.

E-mail address: nkypr2@uky.edu (N. Kyprianou).

<http://dx.doi.org/10.1016/j.molonc.2014.10.014>

1574-7891/© 2014 Federation of European Biochemical Societies. Published by Elsevier B.V. All rights reserved.

1. Introduction

Prostate cancer development and early onset disease is driven by aberrant androgen signaling via the androgen receptor (AR) activity for growth promotion and apoptosis inhibition. Development of metastatic castration-resistant prostate cancer (mCRPC) is a consequence of lack of an apoptotic response to androgen deprivation (Feldman and Feldman, 2001). The treatment landscape for mCRPC has been transformed by the recent FDA approval of the androgen/AR signaling axis inhibitors, built on clinical evidence that AR signaling drives both the therapeutic response and resistance in mCRPC (Chen et al., 2004; Visakorpi et al., 1995). Overexpression of AR detected in CRPC (Feldman and Feldman, 2001; Visakorpi et al., 1995) is able to mediate resistance to anti-androgens (Chen et al., 2004), while point mutations increasing the ligand-binding affinity of AR cause signaling hypersensitivity (Gregory et al., 2001). Promiscuous mutations cause binding flexibility in the ligand-binding domain (LBD) allowing the AR to become activated by adrenal androgens, androgenic metabolites, and anti-androgen therapeutics including enzalutamide and ARN-509 (Dehm et al., 2008; Scher et al., 2012; Tanner et al., 2010; Yilmaz and Christophori, 2009). Moreover, over twenty splicing variants of AR, some lacking LBD, and therefore constitutively active have been identified and associated with progression of CRPC and metastasis (Dehm et al., 2008; Guo et al., 2009; Hu et al., 2009, 2010; Jenster et al., 1995; Sun et al., 2010). AR signaling mediated by truncated AR splice variants (AR-Vs) lacking LBD, is potentially driving the emerging resistance to anti-androgen therapies and CYP17 inhibitors (Cao et al., 2014; Mostaghel et al., 2011; Zhang et al., 2011). Selective loss of AR V7 variant in prostate cancer cells restored sensitivity to enzalutamide (Li et al., 2013).

Taxane-based chemotherapy is a clinically effective treatment for CRPC, by disruption of microtubule dynamics via stabilization of β -tubulin subunits within the microtubule structure, resulting in deregulation of the mitotic spindle assembly. Microtubule formation involves a process of polymerization and depolymerization of α - and β -tubulin heterodimers. Taxanes bind the β -subunit of tubulin, stimulating polymerization into stabilized microtubules that inhibit cell cycle progression leading to G2M arrest and apoptosis (Harrington and Jones, 2011; Vrignaud et al., 2013). Evidence from this laboratory and others established that taxane stabilization of microtubules inhibits the AR translocation into the nucleus, thus preventing the transcriptional activity of AR (Darshan et al., 2011; Zhu et al., 2010). Additionally, taxanes lead to an increase in forkhead box O1 (FOXO1), a transcriptional repressor of AR, consequently resulting in inhibition of ligand-dependent and ligand-independent transcription (Gan et al., 2009). The therapeutic impact of Docetaxel in prohibiting prostate cancer progression and improving survival in patients with advanced disease, has been attributed to utilization of mechanisms previously targeted by androgen deprivation therapy (ADT) (Fitzpatrick and de Wit, 2014; Mistry and Oh, 2013). Despite a proven survival advantage, resistance to Docetaxel develops, leading to disease progression in approximately 7.5 months (Loriot and Fizazi, 2013). Mechanisms implicated in the development of Docetaxel-resistance include overexpression of P-glycoprotein drug efflux pump,

mutational alterations in tubulin expression and induction of epithelial-mesenchymal-transition (EMT) (Fitzpatrick and de Wit, 2014; Loriot and Fizazi, 2013; Puhr et al., 2012).

The process of EMT is an indispensable developmental program for implantation, embryogenesis and organogenesis, but also cancer initiation and progression (Kalluri and Weinberg, 2009). The plasticity afforded to a fully differentiated epithelium, allows individual cells to de-differentiate into mesenchymal-like derivatives, a profound phenotypic transformation representing a reversible process whereby, several rounds of EMT and the reverse process, mesenchymal-epithelial transition (MET) allow for the formation of complex tissues (Moreno-Bueno et al., 2008). EMT becomes a critical venue for epithelial derived tumors to become invasive and rapidly metastasize, with loss of epithelial cell markers (E-cadherin, β -catenin) and gain of mesenchymal markers (N-cadherin, vimentin) at the invasive front being characteristic changes of EMT associated with metastatic spread (Moreno-Bueno et al., 2008).

The N-terminal domain (NTD) of AR is effectively targeted by the novel small molecule, EPI-001/002 (EPI) that interacts with the disordered domain of the AF-1 region and blocks AR transcriptional activity (Andersen et al., 2010; Myung et al., 2013). The functional contribution of the microtubule network and the cytoskeleton to androgen-mediated signaling via navigating AR cellular localization, as well as the consequences of their inhibition by taxanes on AR activity in human prostate cancer have been established (Darshan et al., 2011; Zhu et al., 2010). Considering the compelling evidence that AR variant expression and EMT have both been implicated as mechanisms of resistance to anti-androgens and taxane-based chemotherapy and poor survival (Hornberg et al., 2011; Li et al., 2013; Mostaghel et al., 2011; Puhr et al., 2012; Zhang et al., 2011) and since the association of AR with tubulin occurred via the AR NTD (Zhu et al., 2010), this study investigated the effect of the novel AR NTD antagonist EPI on the sensitivity to taxane treatment *in vitro* and *in vivo* of CRPC harboring the full length AR and the AR splice variants. We found that such a combination strategy effectively suppressed CRPC via navigating cycles of EMT and changes in the cytoskeleton integrity.

2. Materials & methods

2.1. Cell lines

The human prostate cancer cell lines, the castration resistant cell line 22Rv1 and androgen-sensitive LNCaP cells were obtained from American Type Culture Collection (ATCC, Manassas, VA). Cells were maintained in RPMI 1640 (Invitrogen, Grand Island, NY) and 10% fetal bovine serum (FBS), 100units/ml penicillin and 100 μ g/ml streptomycin in a 5% CO₂ incubator at 37 °C. The androgen-independent LNCaP95 cell line (derivative cells from LNCaP) was a generous gift from Dr. Stephen Plymate (University of Washington, Seattle, WA). For experiments examining responses to androgen, cells were seeded in 10% charcoal-stripped serum and were stimulated for 24 h by growth medium containing 1 nM dihydrotestosterone (DHT) (Sigma–Aldrich, St. Louis, MO) or R1881.

2.2. Antibodies

The following antibodies were used for the various experiments. Antibodies against E-cadherin, β -tubulin, Androgen Receptor (N-20), Dynein IC1/2 proteins were purchased from Santa Cruz Biotechnology (Santa Cruz, CA). The antibodies against N-cadherin and CD31 were obtained from AbCam Cell Signaling (Cambridge, UK); antibodies against PARP-1, Vimentin, GAPDH, Snail, cofilin and β -catenin proteins were obtained from Cell Signaling Technology (Danvers, MA).

2.3. Cell viability assay

The effect of the various treatments on prostate cancer cell viability was evaluated using the (Thiazolyl Blue Tetrazolium bromide (MTT) assay). Cells were seeded into 24-well plates and after grown to 60–75% confluency, were treated with vehicle control (DMSO, Sigma–Aldrich, St. Louis, MO), Docetaxel (DOC, 1 μ M), EPI-002 (25 μ M), or combination (1 μ M DOC + 25 μ M EPI-002) in RPMI 1640 with 10% CSS (Charcoal Stripped Serum) for 24 h. At termination of exposure, cells were aspirated and rinsed with PBS then treated with 250 μ l/well MTT (1 mg/ml) for 30 min at 37 °C. After incubation, MTT was aspirated and formazan crystal was solubilized with DMSO. Absorbance was measured at 570 nm using μ Quant Spectrophotometer (Biotech Instruments Inc., Winooski, VT).

2.4. Cell proliferation

Cells seeded into 96-well plates were pre-treated for 1hr with vehicle or EPI-002 (25 μ M). After 16 h, cells were treated with Docetaxel (0.5 μ M) (alone or combination with EPI-002) before addition of R1881 (0.1 nM) or vehicle under serum-free and phenol red-free conditions, and subsequently incubated for 23 h. After pulse-labeling with 10 μ M BrdU (for 2 h), BrdU-labeled cells were identified with the anti-BrdU-POD (Roche). BrdU incorporation was measured at 570 nm using a VersaMax ELISA Microplate Reader (Molecular Devices). The results from three independent experiments performed triplicate were analyzed.

2.5. Western blot analysis

Total cellular protein was extracted from cell pellets by homogenization with RIPA buffer (Cell Signaling Technology, Danvers, MA). Protein samples were loaded into 4%–12% SDS-polyacrylamide gels (Bio-rad, Hercules, CA) and subjected to electrophoretic analysis and blotting. The following antibodies were used against these specific proteins: E-cadherin, N-cadherin, β -tubulin, the AR (N-20), Snail, Vimentin, PARP-1, β -catenin and GAPDH proteins. Membranes were incubated with the specific primary antibody (overnight at 4 °C) and were subsequently exposed to the relevant secondary antibody (90 min, room temperature). For signal detection, membranes were incubated with the Amersham ECL Plus Western Blotting Detection System (Amersham, GE Healthcare, Buckinghamshire, UK) for 5 min and auto-radiographed using X-ray film (Denville Scientific, South Plainfield, NJ). All protein expression bands were normalized to GAPDH expression (used as loading control).

2.6. Quantitative RT-PCR analysis

In vitro samples: RNA was extracted with the Trizol® reagent (Life Technologies, Grand Island, NY) and RNA samples (1 μ g) were subjected to reverse transcription using the Reverse Transcription System (Promega, Madison, WI). TaqMan real time reverse transcriptase-PCR (Life Technologies, Grand Island, NY) analysis of the cDNA samples was conducted in an ABI7700 Sequence Detection System (Applied Biosystems, Inc, Branchburg, NJ), using the following specific primers: for Prostate Specific Antigen (KLK3; Hs02576345_m1), E-cadherin (CDH1; Hs01023894_m1), N-cadherin (CDH2; Hs00983056_m1), Vimentin (VIM; Hs00185584_m1), Snail (SNAI1; Hs00195591_m1), Twist (TWIST1; Hs01675818_s1), UGT2B17 (Hs00854486_sH), and 18S rRNA (4319413E) (Applied Biosystems, Life Technologies, Grand Island, NY). For the qRT-PCR experiments, each sample was analyzed in duplicate and data represent average values from three independent experiments. Numerical data for transcript levels were normalized to 18s rRNA in controls and expressed relative to untreated controls.

2.7. Luciferase reporter gene assays

LNCaP95 cells (1.5×10^5) and 22Rv1 cells (9.5×10^5 in 10% FBS phenol red free RPMI) were transfected with the AR responsive PSA (6.1 kb)-luciferase, probasin (PB)-luciferase and ARR3-luciferase reporters in serum-free media. At 5 h post-transfection, cells were pre-treated with vehicle or EPI-002 (EPI) (25 μ M) for 16 h, and were subsequently exposed to Docetaxel (DOC) (0.5 μ M), or combination of EPI and Docetaxel (EPI + DOC). Cells were incubated with R1881 (1 nM) for 23 h. After 24 h of treatment, cells were lysed and subjected to luciferase reporter activity analyses that were normalized to protein concentrations using the Glomax luminometer (Promega Corporation; Madison, WI). All transfection assays were performed in at least three independent experiments in triplicate wells.

2.8. Immunofluorescent confocal microscopy

Cells were plated (1×10^5) in chamber slides coated with fibronectin (Invitrogen). After 24–48 h, cells were exposed to medium (RPMI 1640 with 10% CSS) in the presence of DHT (1 nM), Docetaxel (DOC: 1 μ M), EPI-002 (EPI: 25 μ M) or in combination of the two agents. Following treatment, cells were fixed in 4% (v/v) paraformaldehyde and permeabilized with 0.1% Triton X-100 in sterile phosphate buffer saline (PBS). Fixed cells were incubated overnight with primary antibody specific for AR (N-20), Dynein IC1/2 and Tubulin, (at 4 °C) with gentle rocking and the appropriate Alexa-Fluor (Life Technologies, Grand Island, NY) fluorescent secondary (1.5 h, room temperature). Slides were mounted using Vectashield mounting medium with DAPI and were visualized using an FV1000 Confocal Microscope (Markey Cancer Center Core, University of Kentucky).

2.9. In vivo tumor targeting studies

All animal experiments were performed in accordance with the guidelines approved by the Animal Care and Use Committee of the University of British Columbia. NOD-SCID mice (6–8 weeks old) were castrated before any drug treatments. At 7

days post-castration, mice were subcutaneously injected with 22Rv1 cells (3×10^6 cells plus Matrigel™ media). Mice were subsequently divided into two groups of 10 mice each: the control group receiving 1% medium/0.1% Tween-20 daily via oral gavage; the other 10 mice in the treatment group received EPI-001 (100 mg/kg twice daily) via oral gavage. EPI-001 had no effect as a monotherapy so when tumors reached approximately 140 mm^3 , 5 mice in each group was intraperitoneally injected (I.P.) with Docetaxel (15 mg/kg) on day 1 and day 5; and the combination treatment of EPI-001 (100 mg/kg twice daily) and Docetaxel (15 mg/kg) for 11 days; Tumors were measured twice a week and the volume calculated by using the formula, length \times height \times width \times 0.5236. Prostate tumor xenografts were harvested two days after the last treatment and tissue specimens were subjected to histopathological analysis. Immunostaining was conducted for the expression and cellular localization of AR, cytoskeleton organization, EMT, vascularity (CD31), and apoptosis (TUNEL, EMD Millipore, Billerica, MA). TUNEL analysis for detection of apoptotic cells was performed as previously (Pu et al., 2009).

2.10. Immunohistochemical analysis

Tissue specimens from human prostate tumor 22Rv1 xenografts were formalin fixed and paraffin-embedded; serial sections (5μ) were subjected to immunohistochemical analysis using antibodies against E-cadherin, N-cadherin, β -tubulin, Androgen Receptor (N-20), cofilin, and CD31. After blocking nonspecific binding (1.5%NGS/TBS-Triton), sections were incubated with primary antibody (overnight, 4°C) and subsequently incubated with biotinylated goat anti-rabbit IgG (2 h, room temperature) and horseradish peroxidase-streptavidin (EMD Millipore, Billerica, MA). Color detection was achieved with SigmaFast 3,3'-Diaminobenzidine tablets (Sigma–Aldrich, St. Louis, MO) and counterstained with haematoxylin. Images were captured via light microscopy ($40\times$ and $100\times$) using an Olympus BX51 microscope (Olympus America, Center Valley, PA). Content and intensity of immuno-reactivity were recorded by two independent observers (S.K.M. and N.K.).

2.11. Statistical analysis

Student's t-test or one-way ANOVA were performed using Graph Pad Prism 6 software to determine the statistical significance of difference between means. All numerical data are presented as Mean \pm Standard error of the mean (SEM). Statistical significance was set at P value <0.05 . ImageJ software was used for calculation of densitometry.

3. Results

3.1. Combination of Docetaxel and EPI maximizes blockade of AR activity and impairs human castration resistant prostate cancer growth in vitro and in vivo

Considering that clinically significant, constitutively active AR splice variants V7 and V567es (Hornberg et al., 2011) regulate the expression of both canonical and a unique subset of

gene targets that are enriched for M-phase cell cycle genes (Cao et al., 2014; Sun et al., 2010), we use two different human prostate cancer cell lines as models, harboring full length functional AR and AR variants to examine the anti-tumor effect of combined targeting of microtubules and AR NTD. The

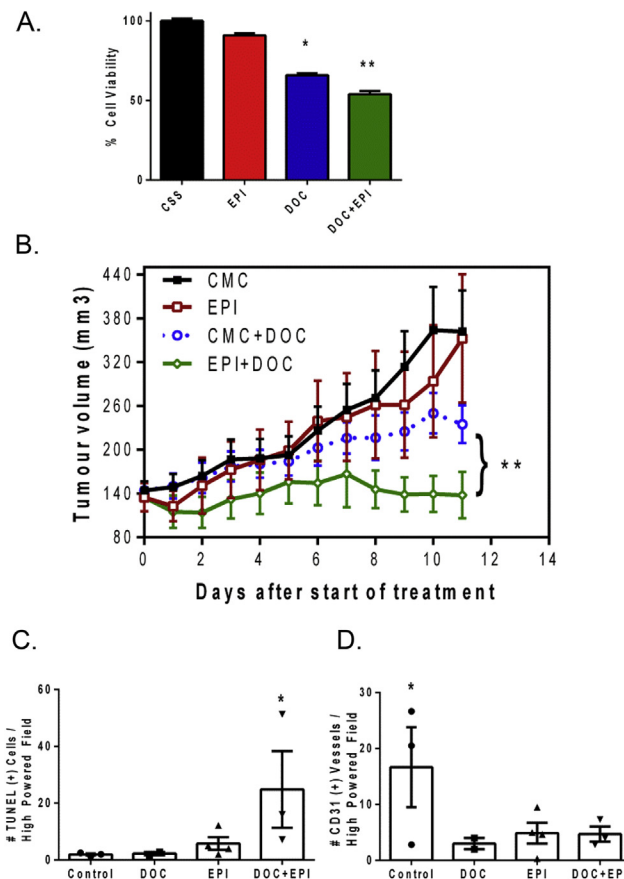


Figure 1 – Combination of an AR NTD inhibitor and Docetaxel impairs growth of castration resistant prostate cancer *in vitro* and *in vivo*. Panel A, the human prostate cancer cells 22Rv1 were treated with EPI (25 μM), or Docetaxel (DOC) (1 μM), as single agents or in combination (DOC + EPI), for 24 h and cell death was assessed on the basis of MTT assay after exposure the drugs. Values represent the average of three experiments (in triplicates) \pm SEM. Statistical significance was set at $P < 0.05$ (*, **). Panel B, *In vivo* anti-tumor action of Docetaxel (microtubule-targeting chemotherapy) and EPI (targeting of the N-terminal domain of AR) in 22Rv1 human prostate cancer xenografts. Palpable tumor-bearing mice were treated with CMC (control), EPI alone (200 mg/kg), Docetaxel alone (DOC) (15 mg/kg), or the combination of the two agents (EPI + DOC) and tumor measurements were conducted as described in “Experimental Procedures” ($n = 5/\text{treatment group}$). Tumor xenografts were surgically excised 2 days after the last treatment (11 days). Error bars represent SEM. ** shows statistically significant difference at $p < 0.05$. Panel C, indicates the quantitative data of apoptosis evaluation the TUNEL assay using serial sections of prostate tumor 22Rv1 xenografts. Panel D, reveals the numerical data of CD31 positivity in serial sections of prostate tumor 22Rv1 xenografts to assess the consequences of various treatments on tumor vascularity. Bars represent the average number of CD-31 positive cells from three different fields per treatment group.

22Rv1 human prostate cancer cells express both functional full-length AR with duplication of exon 3 and substantial levels of constitutively active AR-V7, although they do not exhibit a proliferative response to androgens (Dehm et al., 2008; Guo et al., 2009; Marcia et al., 2010). Treatment of 22Rv1 cells with Docetaxel alone (1 μ M) for 24 h resulted in significant loss of cell viability (Figure 1A). Combination of EPI

with Docetaxel also increased cell death ($P < 0.05$), while EPI as a single agent exerted no significant effect on 22Rv1 cell viability at 24 h.

To examine the anti-tumor effect of EPI alone or in combination with the microtubule-targeting chemotherapy (Docetaxel) *in vivo*, we used 22Rv1 xenografts in mice (castrated for 2-weeks prior to inoculation). As shown on Figure 1B, daily

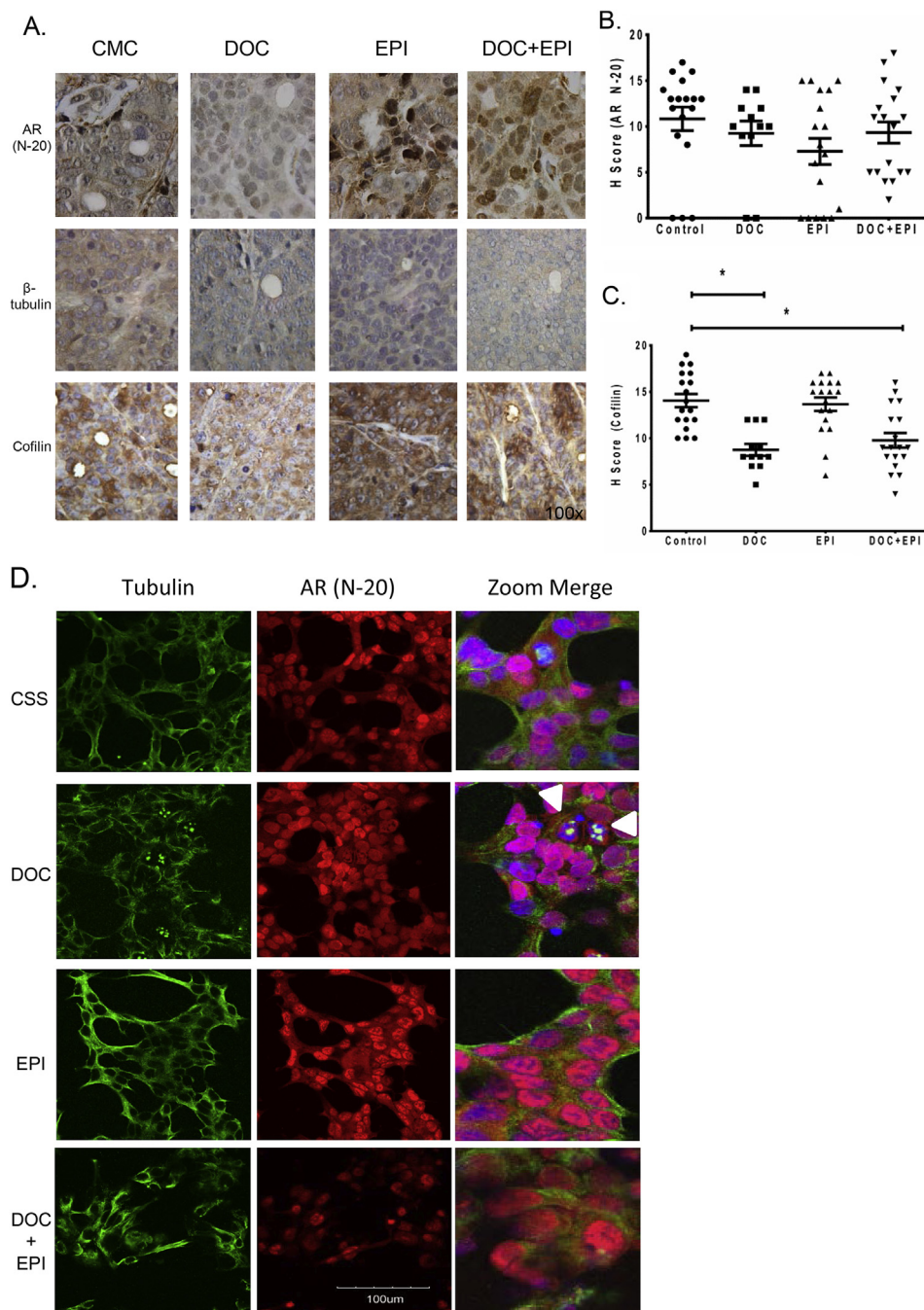


Figure 2 – Effect of microtubule and NTD AR targeting on AR and cytoskeleton in CRPC. Panel A, immuno-reactivity profile for the AR (N-20), β -tubulin (microtubules) and cofilin (actin cytoskeleton as evaluated in paraffin-embedded serial sections from 22Rv1 prostate tumor xenografts; Fig 1B), to determine the effect of treatment on the expression and cellular localization of the specific proteins. Magnification 100 \times . Panel B, numerical data of total AR expression in serial sections before and after the various treatments (based on H-scoring). Panel C, quantitative results of cofilin immuno-reactivity in 22Rv1 xenograft sections (representative images shown on panel A). Docetaxel alone, or in combination with EPI led to a significant decrease in cofilin ($P < 0.05$). Panel D, reveals the fluorescent images of tubulin (green) and AR (red) localization and expression in 22Rv1 cells before (CSS) and after treatment with DOC, EPI, or combination (4 h).

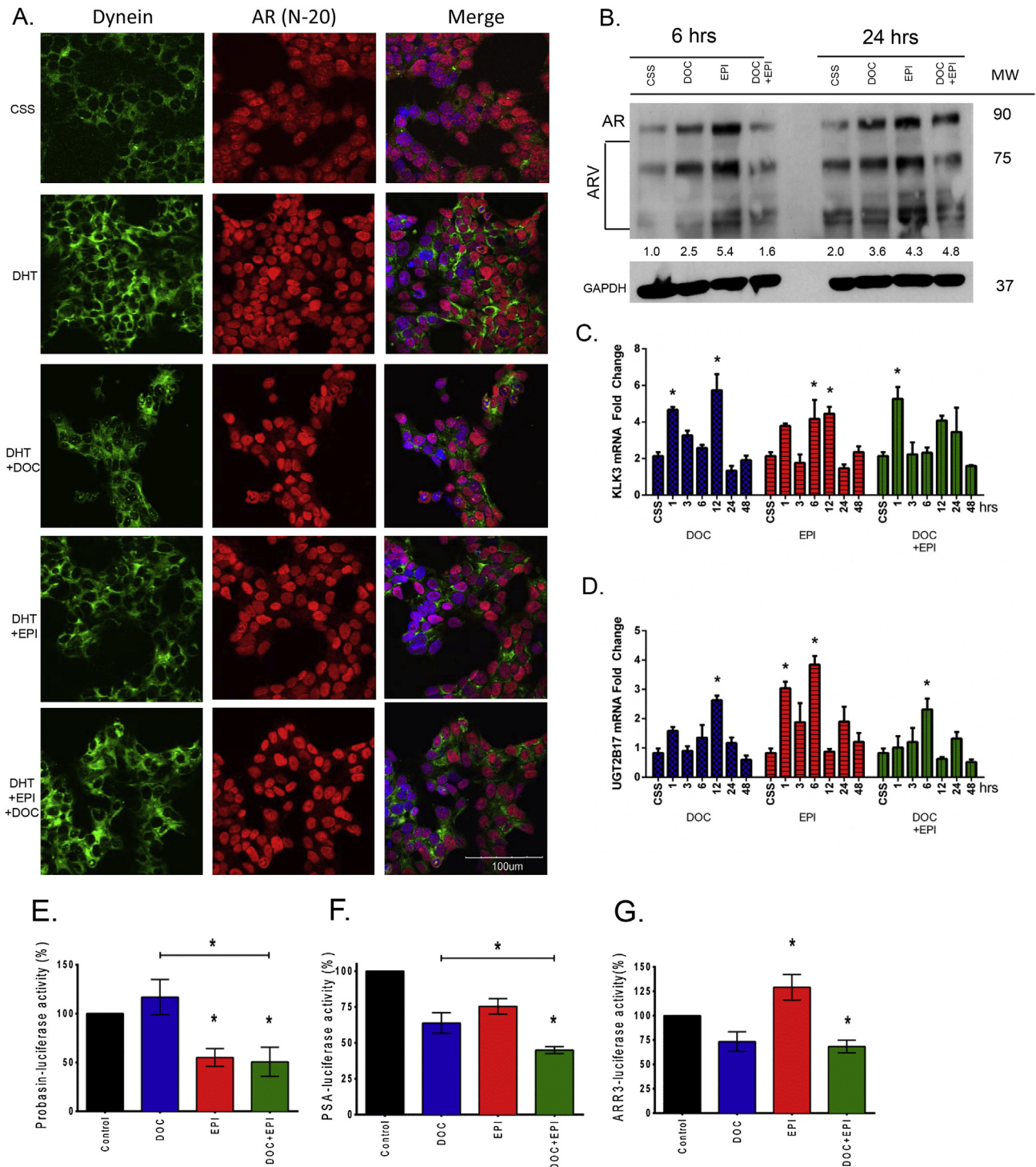


Figure 3 – Effect of targeting microtubules and N-terminal AR on cytosolic protein association and nuclear localization/activity in 22Rv1 prostate cancer cells. Panel A, Confocal image analysis of dynein IC $\frac{1}{2}$ expression and localization in 22Rv1 prostate cancer cells. Cells were exposed to DOC, EPI (as single agents), or in combination (4 h) and were subsequently treated with DHT (1 nM) for 1hr. Cytoplasmic localization of dynein and AR expression were detected using the respective antibodies and serial images are shown. Magnification 200 \times . Panel B, reveals Western blot of AR protein expression profile in 22Rv1 cells after treatment with DOC, EPI or combination, for 6 and 24 h. Control cells, exposed to CSS medium. GAPDH was used as a loading control. MW of the full length AR and the variants are shown on left and densitometry of full length AR indicated below blot. Panels C and D, reveal the RT-PCR analysis of PSA/CLK3 mRNA expression (FL-AR target gene) and UGT2B17 mRNA expression (AR V7 target gene) respectively in 22Rv1 human prostate cancer cells in response to treatments. Numerical values are the mean of three measurements for a single gene performed in triplicate \pm SEM. Panels E, F and G, indicate the results for the transcriptional reporter assays in 22Rv1 cells. Cells were transiently transfected with PB-luciferase (E), PSA (6.1 kb)-luciferase (F), or ARR3-Luc reporters (G) and pre-treated with EPI, DOC, or combination (EPI + DOC) prior to incubation with R1881. Luciferase activity is represented as percentage of vehicle control activity in response to androgen. Bars represent SEM of three independent experiments.

treatment with the AR N-terminal inhibitor EPI (200 mg/kg), did not result in a significant growth inhibition of the 22Rv1 xenografts compared to vehicle control. The combination treatment of Docetaxel and EPI led to a significant suppression of CRPC tumor growth compared to either single treatment modality or untreated controls (Figure 1B) ($P < 0.05$). This dramatic prostate cancer xenograft eradication was associated with a significant increase in the number of apoptotic cells in the combination treated tumor xenografts compared to untreated control or single treatment arms, as evaluated with the TUNEL assay (Figure 1C). Assessment of the tumor vascularity based on the CD31 immuno-reactivity in xenograft tumors demonstrated a significant decrease in tumor vascularity in response to EPI and Docetaxel combination compared to untreated controls (Figure 1D; Supplemental Figure S1).

In response to Docetaxel, there was an apparent decrease in the AR immuno-reactivity in the 22Rv1 CRPC xenografts (Figure 2A). Quantitative evaluation of AR positivity and cellular localization however, did not reveal any significant changes after any of the treatments relative to untreated control (Figure 2B). As expected, treatment of mice with Docetaxel led to reduction in tubulin expression in the prostate tumor xenografts that was further enhanced by the combination treatment of Docetaxel and EPI. Quantitative analysis of cofilin immuno-reactivity revealed a significant decrease of this critical cytoskeleton protein in response to Docetaxel and the combination treatment, compared to untreated control (Figure 2C). To further interrogate these protein changes elicited by the combination treatment of Docetaxel and the NTD AR targeting, we use confocal microscopy in 22Rv1 cells *in vitro*. As shown on Figure 2 (panel D), treatment with Docetaxel alone (for 4 h), led to a marked reduction in β -tubulin expression and mitotic arrest (merged image, arrow heads) in CRPC. Prostate cancer cells exhibiting microtubule stabilization appear to have some cytoplasmic AR localization in 22Rv1 cells (Figure 2D). Consistent with the *in vivo* xenograft data (Figure 2A), there were no significant changes in the expression of AR after Docetaxel treatment (as single agent or in combination with EPI) compared to untreated control cells (Figure 2D).

Docetaxel caused a significant loss in body weight compared to animals treated with vehicle control ($86\% \pm 3.0\%$ vs $102\% \pm 1.3\%$, $p = 0.0011$), while EPI had no significant effect ($98\% \pm 1.3\%$, $p = 0.6088$). The body weight of mice treated with EPI in combination with Docetaxel was also significantly lower than that obtained for the vehicle control ($86\% \pm 5.4\%$, $p = 0.0156$), but not significantly different than the weight measurements from mice treated with Docetaxel monotherapy ($p = 0.9529$). Thus the combination treatment of EPI and Docetaxel does not appear to induce toxicity beyond that obtained from Docetaxel alone.

3.2. Impact of AR variants on taxane-mediated AR trafficking

The existence of AR variants capable of androgen-independent signaling may be critical in dictating the therapeutic response to taxanes. It was recently shown that the AR variant core consisting of the AR NTD and DNA-binding

domain is sufficient for nuclear localization and androgen-independent transcriptional activation of AR target genes (Chan et al., 2012). We subsequently examined the effect of EPI and Docetaxel on the expression and cellular localization of the AR, as well as tubulin, in the 22Rv1 cells in the presence of DHT. An apparent stabilization of microtubule structures and a decrease in tubulin levels were detected in response to the combination treatment of Docetaxel and EPI (Supplementary Figure 2A). Figure 3 (panel A), reveals fluorescent images of the 22Rv1 prostate cancer cells in response to Docetaxel or EPI (as single agents), or the combination of the two agents. A modest effect of Docetaxel on androgen-induced nuclear AR translocation was observed after 4 h of treatment. This was confirmed by subcellular fractionation analysis revealing that Docetaxel treatment reduced the nuclear presence of full length AR, without causing marked changes in AR variants (nuclear vs cytosolic levels) (Supplementary Figure S2B). This is in contrast to the ability of Docetaxel and also EPI (given as single agents or in combination) to promote the cytoplasmic sequestration of AR from the nuclei in the androgen-sensitive LNCaP cells, harboring a full length AR (Supplementary Figure S3A). This impact on AR nuclear translocation by taxane and EPI-docetaxel combination in LNCaP cells was translated into a significant inhibitory effect against cell viability (Supplementary Figure S3). Western blot analysis revealed that within 6 h of treatment with EPI there was an increase in protein levels of both full-length and variant AR compared to untreated 22Rv1 cells that was suppressed by the combination treatment of EPI with Docetaxel (Figure 3B).

Dynein is a microtubule-traversing motor protein capable of efficiently facilitating nuclear transport of cytoplasmic proteins, that was previously shown to navigate AR trafficking along the microtubules and its nuclear translocation, towards induced transcriptional activity (Darshan et al., 2011). We thus examined the expression and cellular localization of dynein in 22Rv1 cells in response to the various treatments and its colocalization with AR. Androgens (DHT) increase expression of dynein and this correlates with increased AR nuclear translocation (Figure 3A; merged image). In response to Docetaxel, there was a marked alteration in dynein localization as detected by confocal microscopy (appearing as punctate sequestration), while EPI alone did not have any effect on dynein distribution/localization (Figure 3A). In marked contrast in the androgen-sensitive LNCaP cells (full length AR), treatment with Docetaxel alone or in combination with EPI, in the presence of DHT, resulted in diffuse cellular localization of dynein (Supplementary Figure S3A).

3.3. Differential effect of taxane and EPI treatment on AR vs AR-V7 target genes

To determine the impact of treatment on the functional activity of AR, the temporal induction of AR regulated genes was evaluated in 22Rv1 cells in response to Docetaxel, EPI or the combination treatment. Prostate-specific antigen (PSA/KLK3) is a gene target for the full length AR and UGT2B17 is a gene target for AR V7 variant. There was a significant increase in KLK3 mRNA expression in response to treatment (within an hour) with Docetaxel monotherapy and combination therapy

(Figure 3C) ($P < 0.05$). There was no significant effect on KLK3 expression, in response to either EPI or Docetaxel given as single agents, or in combination (after 24 and 48 h), relative to untreated levels. A transient increase in UGT2B17 mRNA levels was detected within 1–6 h of treatment with EPI (Figure 3D). After longer treatment periods (12–48 h), upregulation of UGT2B17 in response to either EPI or combination with Docetaxel, was not sustained.

We subsequently investigated whether the combination treatment of Docetaxel and EPI, exerts an enhanced inhibitory effect of AR transcriptional activity, using three AR-driven reporter gene constructs in the 22Rv1 cells. The probasin (PB, –286/+28) reporter gene construct is the natural promoter that contains two functional androgen response elements (AREs), that comprise the androgen response region (ARR). The PSA (6.1 kb) reporter gene construct is also a natural reporter with several AREs in both the enhancer and promoter regions. The ARR3 is an artificial reporter with 3 repeats of the PB ARR in front of a minimal thymidine kinase promoter. The data shown on Figure 3, demonstrate that treatment with EPI led to significant inhibition of the androgen-induced PB-luciferase and PSA-luciferase reporters (panels E and F respectively), while unexpectedly increased the activity of the synthetic ARR3 reporter (Figure 3G) ($P < 0.05$); this finding resonates with the increase in AR protein levels by EPI (Figure 3B). The combination of Docetaxel and EPI consistently achieved a significant inhibitory effect for all three AR-driven reporters in 22Rv1 cells (Figure 3, panels E–G).

To validate the enhanced anti-tumor potency of the combination approach of taxanes and EPI against another androgen-insensitive prostate cancer cell line, the proliferative response of LNCaP95 human prostate cancer cells that express functional full-length AR and the AR-V7 variant was investigated (Hu et al., 2012). We found that EPI treatment alone or in combination with Docetaxel significantly inhibited cell proliferation in LNCaP95 cells, while Docetaxel as a single agent resulted in a 25% decrease in cell proliferation (Figure S5A). Furthermore analysis of the AR transcriptional activity, demonstrated that treatment of LNCaP95 cells with either EPI or Docetaxel given as single agents significantly inhibited the androgen-induced activity for all three reporters (Figure S5, panels B, C and D), prior to manifestation of cell death (Figure 4E). Consistent with the findings in 22Rv1 cells, the combination of Docetaxel and EPI resulted in maximal blockade of AR transcriptional activity in LNCaP95 cells.

3.4. Role of EMT in therapeutic response of CRPC to combined targeting of AR NTD and microtubules

The recently reported association of AR variants with clinical prostate cancer progression and therapeutic resistance to taxanes and anti-androgens (Cao et al., 2014; Li et al., 2013; Mostaghel et al., 2011; Zhang et al., 2011) may be driven by induced EMT. To assess the impact of AR NTD targeting on the EMT phenotype of prostate tumor epithelial cells after Docetaxel treatment, we subsequently conducted an expression profile of key EMT effectors in 22Rv1 cells following single agent or combination treatment. Treatment with EPI led to a marked increase of N-cadherin protein levels compared to

the untreated control cells (Figure 4A); this N-cadherin upregulation was attenuated by combination with Docetaxel. By 24 h-post treatment the key phenotypic change of elevated N-cadherin associated with EMT induction was restored to control levels (Supplementary Figure S4). No significant changes in levels of Twist, E-cadherin or N-cadherin temporal expression were detected. A modest decrease in the cytoskeleton protein, cofilin was evident after 24 h of DOC or EPI monotherapy.

The EMT landscape was subsequently interrogated in the *in vivo* setting of 22Rv1 prostate tumor xenografts (from Figure 1B). E-cadherin expression was increased in response to both Docetaxel and EPI given as single agents, while N-cadherin levels were decreased compared to the untreated controls (Figure 4B) consistent with the phenotypic reversion of EMT to MET in prostate tumor epithelial cells. Interestingly, the combination treatment led to an apparent decrease in E-cadherin and upregulation of N-cadherin protein levels (EMT). Tissue levels of vimentin were increased after treatment with EPI or Docetaxel given as single agents, an effect that was blocked by the combination treatment (Figure 4B; Supplementary S1C).

The temporal changes in gene expression for EMT regulators were interrogated by analysis of mRNA expression levels by qRT-PCR. The results summarized in Figure 4 indicate that consistent with EPI increasing levels of N-cadherin protein at 6 h, levels of N-cadherin mRNA were also elevated within the same period of exposure to EPI, compared to levels observed for CSS control (Figure 4C). Upregulation of mRNA for vimentin and E-cadherin was also detected within 6 h of treatment with EPI. After longer treatment periods (12, 24 and 24 h), the levels for both proteins were restored to levels comparable to the controls. A significant increase in N-cadherin mRNA was detected in response to Docetaxel (as single agent) at 1 and 3 h, but with no effect on vimentin mRNA (Figure 4C). The combination treatment of EPI and Docetaxel for 24 h resulted in a significant increase in the levels of mRNA for both N-cadherin and vimentin. A significant induction of Snail mRNA, a transcriptional repressor for E-cadherin, was observed in response to both monotherapies and this was further increased response to the combination of Docetaxel with EPI (Figure 4C). Within the first hour of combination treatment, there was a significant induction in Twist gene expression (Figure 4C). Elevated expression of N-cadherin occurs in response to attenuated AR transcriptional activity or reduced levels of expression of AR (Jennbacken et al., 2010; Tanaka, 2010). Thus, these findings support the “programming” of EMT by the AR N-terminal inhibitor, to potentially drive the sensitivity/resistance of CRPC 22Rv1 cells to microtubule-targeting taxane-based chemotherapy (Figure 4D).

4. Discussion

Therapeutic response durations to androgen-depletion in advanced metastatic prostate cancer are variable and prostate tumors nearly always become resistant and ultimately lethal. Diverse mechanisms have been implicated in driving aberrant AR function, including intra-tumoral synthesis of androgens from inactive precursors, increased AR expression, truncated

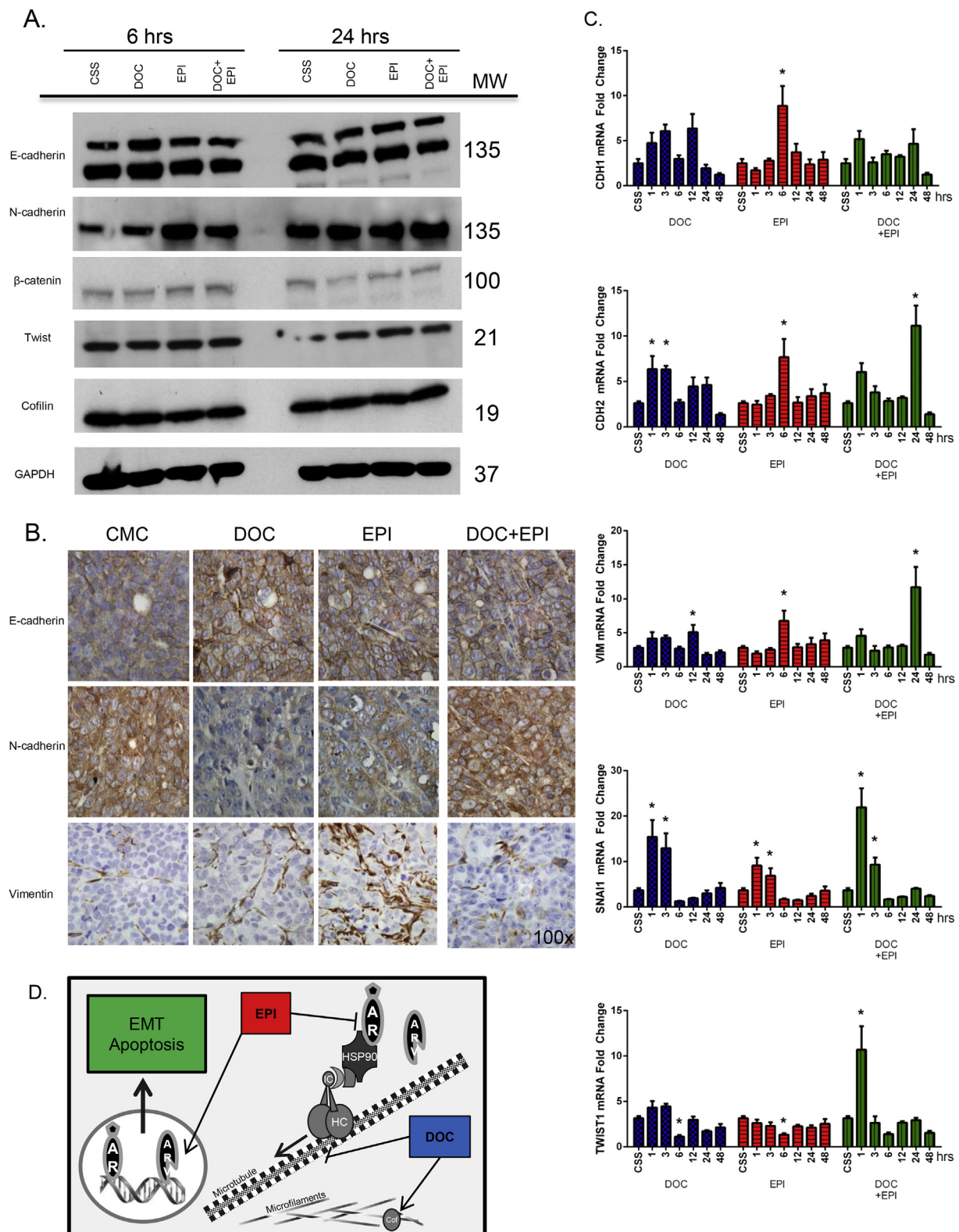


Figure 4 – Impact of AR Variant on EMT in CRPC 22Rv1 Cells in Response to Combination Targeting of the AR NTD and Microtubules. Panel A, Western blot analysis of critical EMT regulator proteins after 6 and 24 h of treatment of 22Rv1 cells with DOC, EPI or combination. Expression levels for E-cadherin, N-cadherin, β-catenin, Twist and the actin organization protein, cofilin are shown. GAPDH was used as a loading control. The MW of individual proteins is shown on the right (kDa). Panel B, serial sections of 22Rv1 prostate tumor xenografts from untreated control (CMC) and treated tumor-bearing mice (DOC, EPI, or combination, obtained as in Fig.1B), were subjected to immunohistochemical analysis for the EMT markers E-cadherin, N-cadherin and vimentin. Magnification 100x. Panel C reveals the temporal analysis of gene expression of EMT regulators. 22Rv1 prostate cancer cells were treated with DOC, EPI or the combination (1, 3, 6, 12, 24 and

AR with constitutive activity, ligand-independent activation of AR signaling and alterations in nuclear receptor co-activators (Debes and Tindall, 2004; Knudsen and Penning, 2010). Novel pharmacologic targeting of these mechanisms has provided some validation in the clinical setting in the treatment of CRPC, such as those that require the AR ligand-binding domain (Lunardi et al., 2013).

A new paradigm has emerged in therapeutic targeting of microtubule-mediated androgen signaling in prostate cancer, by growing evidence indicating that taxane-induced stabilization of microtubules inhibits the nuclear translocation of the androgen-AR complex and impairs AR transcriptional activation (Darshan et al., 2011; Gan et al., 2009; Zhu et al., 2010). Our present findings indicate that Docetaxel treatment causes only a modest inhibition of the AR nuclear localization, although there was a significant suppression of AR-transcriptionally activated gene expression, in the 22Rv1 CRPC prostate cancer cells. Considering that these cells express a mixture of the full-length AR as well as the AR variants, this was not entirely unexpected. These results gain mechanistic support from recent evidence by Chan and colleagues demonstrating that AR splice variants activate AR target genes and promote prostate cancer growth independent of canonical AR nuclear localization signal (Chan et al., 2012). More recently it was reported that the nuclear accumulation and transcriptional activity of AR V7 variant was not affected by microtubule-targeting chemotherapy (Thadani-Mulero et al., 2014), in full support of our findings. Thus one may argue that while nuclear AR localization is functionally critical for controlling AR (full length) transcriptional activation of target genes in androgen-dependent prostate cancer, other distinct pathways may exist to regulate the AR variants nuclear translocation in CRPC, thus driving therapeutic resistance to microtubule-targeting chemotherapy and/or anti-androgens. Interestingly enough, the AR V7 lacks the hinge region which facilitates microtubule targeting and navigates AR nuclear trafficking (Tanner et al., 2010; Thadani-Mulero et al., 2014). Our findings on the modest effect of microtubule-targeting treatment on AR V7 transcriptional activity are in accord with the above mechanistic evidence.

Our observations indicate that the microtubule motor protein, dynein can efficiently facilitate the cytoplasmic AR trafficking along the microtubules and its nuclear translocation in the presence of androgens, resonates with previous reports (Darshan et al., 2011). In addition, we found that the status of the AR dictates the cellular response Docetaxel treatment (alone or in combination with EPI) in terms of changes in dynein localization causing punctate sequestration in nuclear and cytoplasmic fractions in CRPC 22RV1 cells (variant AR), while in the androgen-sensitive LNCaP cells (full length AR), treatment leads to massive distribution of dynein throughout the cytosol, promoting the nuclear export of AR (Figure 4D). Mechanistically, a differential association with microtubules and the dynein motor protein has been shown for the

clinically significant splice variants ARv567es and AR V7, with the AR V7 unable to interact with dynein and ultimately not having an effect on AR nuclear transport and transcriptional activity (Thadani-Mulero et al., 2014). This evidence together with our present results, suggest that dynein may be engaging additional cytoplasmic partners such as HSP90, as well as cytoskeleton modulators to generate a new dynamic of interactions with full length AR versus AR variants, effective targeting of which can potentially bypass cross-resistance to Docetaxel and anti-androgens in advanced prostate cancer.

The present study demonstrates that combination of the microtubule-targeting agent, Docetaxel with targeting the AR NTD with EPI leads to enhanced anti-tumor action possibly via changes in the EMT landscape and the cytoskeleton of prostate cancer cells harboring AR variants. A functional significance of the EMT process in therapeutic response to microtubule-targeting is supported by the recently reported association between reduced E-cadherin expression and Docetaxel-resistance in prostate cancer cells (Puhr et al., 2012). Reduced E-cadherin expression promotes loss of cell adhesion, cell polarization, and gain of cell migration, which leads to invasion and metastases (Yang and Weinberg, 2008; Yilmaz and Christophori, 2009). Moreover there is growing clinical evidence implicating EMT as a cellular mechanism conferring therapeutic resistance, development of metastases, and contributing to patient mortality (Puhr et al., 2012). Considering that interference with the androgen/AR signaling axis is associated with EMT induction (Matuszak and Kyprianou, 2011; Sun et al., 2011; Zhu and Kyprianou, 2010), Docetaxel administration prior to androgen deprivation may result in improved therapeutic outcomes via navigating the EMT-MET cycling, towards cytoskeleton remodeling and sensitizing prostate tumor cells to androgen-depletion mediated apoptosis. An alternative mechanistic scenario is that mutations in tubulin may affect the binding sites of taxanes leading to therapeutic resistance. One may argue that when taxanes are structurally unable to effectively bind tubulin, the microtubules can no longer become stabilized, an effect that fails to elicit disruption of cell cycle progression, and consequentially the AR is free for a nuclear translocation (schematically illustrated on Figure 4D). Treatment of CRPC with EPI, an ARNTD inhibitor, leads to decreased transcriptional activity of both full-length AR and constitutively active truncated variants (Andersen et al., 2010; Myung et al., 2013) and is thereby an attractive target for prohibiting AR from the nucleus to remain in the cytoplasm using taxanes as a combination therapy.

4.1. Conclusions

In summary, the present pre-clinical studies demonstrate that the combination strategy of targeting tubulin (by taxane chemotherapy) -and the NTD of AR variants association (by EPI) and cellular localization can impair CRPC by reversing

48 h) and mRNA expression was analyzed by RT-PCR. The gene expression profile of mRNA for the EMT effectors, E-cadherin (CDH1), N-cadherin (CDH2), and vimentin (VIM), as well as for the transcriptional regulators SNAIL1 and Twist, in response to treatments is shown. Values represent the mean \pm SEM of duplicate measurements from three independent experiments; (*) denotes statistical significance at $p < 0.05$. Panel D, schematic diagram projecting the potential interactions of AR with cytoplasmic proteins (dynein, tubulin, cofilin) that may control its nuclear translocation and transcriptional activity of target genes, mediating EMT and apoptosis in CRPC cells.

EMT and navigating EMT-MET cycling. These findings provide a new insight into a potential mechanism for overcoming cross-resistance driven by differential status, and activity of AR, depending on its nuclear/cytosolic localization. Further understanding of the mechanisms of aberrant activation of AR and the distinct transcriptome of AR variants compared to full length wild-type AR, is central to the optimization of therapeutic targeting of CRPC and of major significance in patients who failed Docetaxel therapy. Ongoing studies focus on interrogation of the functional relationships between dynein and other partners such as HSP90, facilitating interactions between AR variants and tubulin in the cytoplasm of prostate cancer cells and the impact on cancer cell migration and invasion in CRPC (Figure 4D).

Author contributions

S.K.M., M.D.S. and N.K. designed research; S.K.M. and C.A.B. performed research; C.A.B. and M.D.S. contributed new reagents; S.K.M., C.A.B., M.D.S., and N.K. analyzed data; and S.K.M., M.D.S. and N.K. wrote the manuscript.

Conflicts of interest

Marianne D. Sadar and Carmen A. Banuelos own ESSA Pharma Inc stock. There are no conflicts by the other authors.

Acknowledgments

This was supported by grants from the National Institutes of Health, (NIDDK, R01-00491815), the James F. Hardyman Endowment (NK); National Cancer Institute (2R01 CA105304), the Canadian Institutes of Health Research (MOP79308), the US Army Medical Research and Materiel Command Prostate Cancer Research Program (W81XWH-11-1-0551) (MDS). The authors are thankful to Jun Wang (British Columbia Cancer Agency) and Dr. Hong Pu (University of Kentucky) for their expert assistance with the *in vivo* xenograft studies and immunohistochemical analysis of prostate tumors.

Appendix A.

Supplementary data

Supplementary data related to this article can be found at <http://dx.doi.org/10.1016/j.molonc.2014.10.014>.

REFERENCES

Andersen, R.J., Mawji, N.R., Wang, J., Wang, G., Haile, S., Myung, J.-K., Watt, K., Tam, T., Yang, Y.C., Banuelos, C.A., Williams, D.E., McEwan, I.J., Wang, Y., Sadar, M.D., 2010. Regression of castrate-recurrent prostate cancer by a small-molecule inhibitor of the amino-terminus domain of the androgen receptor. *Cancer Cell* 17, 535–546.

Cao, B., Qi, Y., Zhang, G., Xu, D., Zhan, Y., Alvarez, X., Guo, Z., Fu, X., Plymate, S.R., Sartor, O., Zhang, H., Dong, Y., 2014. Androgen receptor splice variants activating the full length receptor in mediating resistance to androgen-directed therapy. *Oncotarget* 5, 1635–1645.

Chan, S.C., Li, Y., Dehm, S.M., 2012. Androgen receptor splice variants activate androgen receptor target genes and support aberrant prostate cancer cell growth independent of canonical androgen receptor nuclear localization signal. *J. Biol. Chem.* 287, 19736–19749.

Chen, C.D., Welsbie, D.S., Tran, C., Baek, S.H., Chen, R., Vessella, R., Rosenfeld, M.G., Sawyers, C.L., 2004. Molecular determinants of resistance to antiandrogen therapy. *Nat. Med.* 10, 33–39.

Darshan, M.S., Loftus, M.S., Thadani-Mulero, M., Levy, B.P., Escuin, D., Zhou, X.K., Gjyrezii, A., Chanel-Vos, C., Shen, R., Tagama, S.T., Bander, N.H., Nanus, D.M., Giannakakou, P., 2011. Taxane-induced blockade to nuclear accumulation of the androgen receptor predicts clinical responses in metastatic prostate cancer. *Cancer Res.* 71, 6019–6029.

Debes, J.D., Tindall, D.J., 2004. Mechanisms of androgen-refractory prostate cancer. *N. Engl. J. Med.* 351, 1488–1490.

Dehm, S.M., Schmidt, L.J., Heemers, H.V., Vessella, R.L., Tindall, D.J., 2008. Splicing of a novel androgen receptor exon generates a constitutively active androgen receptor that mediates prostate cancer therapy resistance. *Cancer Res.* 68, 5469–5477.

Feldman, B.J., Feldman, D., 2001. The development of androgen-independent prostate cancer. *Nat. Rev. Cancer* 1, 34–45.

Fitzpatrick, J.M., de Wit, R., 2014. Taxanes mechanisms of action: potential implication for treatment sequencing in metastatic castration-resistant prostate cancer. *Eur. Urol.* 65, 1198–1204.

Gan, L., Chen, S., Wang, Y., Watahiki, A., Bohrer, L., Sun, Z., Wang, Y., Huang, H., 2009. Inhibition of the androgen receptor as a novel mechanism of taxol chemotherapy in prostate cancer. *Cancer Res.* 69, 8386–8394.

Gregory, C.W., Johnson, R.T., Mohler, J.L., French, F.S., Wilson, E.M., 2001. Androgen receptor stabilization in recurrent prostate cancer is associated with hypersensitivity to low androgen. *Cancer Res.* 61, 2892–2898.

Guo, Z., Yang, X., Sun, F., Jiang, R., Linn, D.E., Chen, H., Chen, H., Kong, X., Melamed, J., T, C.G., Kung, H.-J., Brodie, A.M.H., Edwards, J., Qiu, Y., 2009. A novel androgen receptor splice variant is up-regulated during prostate cancer progression and promotes androgen depletion-resistant growth. *Cancer Res.* 69, 2305–2313.

Harrington, J.A., Jones, R.J., 2011. Management of metastatic castration-resistant prostate cancer after first-line docetaxel. *Eur. J. Cancer* 47, 2133–2142.

Hornberg, E., Ylitalo, E.B., Crnalic, S., Antti, H., Stattin, P., Widmark, A., Bergh, A., Wikstrom, P., 2011. Expression of androgen receptor splice variants in prostate cancer bone metastases is associated with castration-resistance and short survival. *PLoS One* 6, e19059.

Hu, R., Dunn, T.A., Wei, S., Isharwal, S., Veltri, R.W., Humphreys, E., Han, M., Partin, A.W., Vessella, R.L., Isaacs, W.B., Bova, G.S., Luo, J., 2009. Ligand independent androgen receptor variants derived from splicing of cryptic exons signify hormone refractory prostate cancer. *Cancer Res.* 69, 16–22.

Hu, R., Isaacs, W.B., Luo, J., 2010. A snapshot of the expression signature of androgen receptor splicing variants and their distinctive transcriptional activities. *Prostate* 71, 1656–1667.

Hu, R., Lu, C., Mostaghel, E.A., Yegnasubramanian, S., Gurel, M., Tannahill, C., Edwards, J., Isaacs, W.B., Nelson, P.S., Bluemn, E., Plymate, S.R., Luo, J., 2012. Distinct transcriptional programs mediated by the ligand-dependent full-length androgen receptor and its splice variants in

- castration-resistance prostate cancer. *Cancer Res.* 72, 3457–3462.
- Jennbacken, K., Tesan, T., Wang, W., Gustavsson, H., Damber, J.E., Welen, K., 2010. N-cadherin increases after androgen deprivation and is associated with metastasis in prostate cancer. *Endocr. Relat. Cancer* 17, 469–479.
- Jenster, G., van der Korput, H.A.G.M., Trapman, J., Brinkmann, A.O., 1995. Identification of two transcription activation units in the N-terminal domain of the human androgen receptor. *J. Biol. Chem.* 270, 7341–7346.
- Kalluri, R., Weinberg, R.A., 2009. The basics of epithelial-mesenchymal transition. *J. Clin. Invest.* 119, 1420–1428.
- Knudsen, K.E., Penning, T.M., 2010. Partners in crime: deregulation of AR activity and androgen synthesis in prostate cancer. *Trends Endocrin. Metab.* 21, 315–324.
- Li, Y., Chan, S.C., Brand, L.J., Hwang, T.H., Silverstein, K.A.T., Dehm, S.M., 2013. Androgen receptor splice variants mediate enzalutamide resistance in castration-resistant prostate cancer cell lines. *Cancer Res.* 73, 483–489.
- Loriot, Y., Fizazi, K., 2013. Taxanes: still a major weapon in the armamentarium against prostate cancer. *Eur. Urol.* 63, 983–985.
- Lunardi, A., Ala, U., Epping, M.T., Salmena, L., Clohessy, J.G., Webster, K.A., Wang, G., Mazzucchelli, R., Bianconi, M., Stack, E.C., Lis, R., Patnaik, A., Cantley, L.C., Bubley, G., Cordon-Cardo, C., Gerald, W.L., Montironi, R., Signoretti, S., Loda, M., Nardella, C., Pandolfi, P.P., 2013. A co-clinical approach identifies mechanisms and potential therapies for androgen deprivation resistance in prostate cancer. *Nat. Genet.* 45, 747–755.
- Marcia, G., Erdmann, E., Lapouge, G., Siebert, C., Barthelemy, P., Duclos, B., Bergerat, J.-P., Geraline, J., Kurtz, J.-E., 2010. Identification of novel truncated androgen receptor (AR) mutants including unreported pre-mRNA splicing variants in the 22Rv1 hormone-refractory prostate cancer (PCa) cell line. *Hum. Mutat.* 31, 74–80.
- Matuszak, E.A., Kyprianou, N., 2011. Androgen regulation of epithelial-mesenchymal transition in prostate tumorigenesis. *Expert Rev. Endocrin. Metabol.* 6, 469–482.
- Mistry, S.J., Oh, W.K., 2013. New paradigms in microtubule-mediated endocrine signaling in prostate cancer. *Mol. Cancer Ther.* 12, 555–566.
- Moreno-Bueno, G., Portillo, F., Cano, A., 2008. Transcriptional regulation of cell polarity in EMT and cancer. *Oncogene* 27, 6958–6969.
- Mostaghel, E.A., Marck, B.T., Plymate, S.R., Vessella, R.L., Balk, S., Matsumoto, A.M., Nelson, P.S., Montgomery, R.B., 2011. Resistance to CYP17A1 inhibition with abiraterone in castration-resistant prostate cancer: induction of steroidogenesis and androgen receptor splice variants. *Clin. Cancer Res.* 17, 5913–5925.
- Myung, J.-K., Banuelos, C.A., Fernandez, J.G., Mawji, N.R., W, J., Tien, A.H., Yang, Y.C., Tavakoli, I., Haile, S., Watt, K., McEwan, I.J., Plymate, S.R., Andersen, R.J., Sadar, M.D., 2013. An androgen receptor N-terminal domain antagonist for treating prostate cancer. *J. Clin. Invest.* 123, 2948–2960.
- Pu, H., Collazo, J., Jones, E., Gayheart, D., Sakamoto, S., Vogt, A., Mitchell, B., Kyprianou, N., 2009. Dysfunctional TGF- β Receptor II accelerates prostate cancer tumorigenesis in TRAMP mouse model. *Cancer Res.* 69, 7366–7374.
- Puhr, M., Hoefer, J., Schafer, G., Erb, H.H., Oh, S.J., Klocker, H., Heidegger, I., Neuwirt, H., Cullig, Z., 2012. Epithelial-to-mesenchymal transition leads to docetaxel resistance in prostate cancer and is mediated by reduced expression of miR-200c and miR-205. *Am. J. Pathol.* 181, 2188–2201.
- Scher, H.I., Fizazi, K., Saad, F., Taplin, M.-E., Sternberg, C.N., Miller, K., De Wit, R., Mulders, P., Hirmand, M., Selby, B., de Bono, J.S., 2012. Effect of MDV3100, an androgen receptor signaling inhibitor (ARSI) on overall survival in patients with prostate cancer postdocetaxel: results from the phase III AFFIRM study. *J. Clin. Oncol.* 30.
- Sun, S., Sprenger, C.C.T., Vessella, R.L., Haugk, K., Soriano, K., Mostaghel, E.A., Page, S.T., Coleman, I.M., Nguyen, H.M., Sun, H., Nelson, P.S., Plymate, S.R., 2010. Castration resistance in human prostate cancer is conferred by a frequently occurring androgen receptor splice variant. *J. Clin. Invest.* 120, 2715–2730.
- Sun, Y., Wang, B.-F., Leong, K.G., Yue, P., Li, L., Jhunjhunwala, C.D., et al., 2011. Androgen deprivation causes epithelial-mesenchymal transition on the prostate implications for androgen-deprivation therapy. *Cancer Res.* 72 (2), 527–536.
- Tanaka, H., Kono, E., Tran, C.P., Miyazaki, H., Yamashiro, J., Shimomura, T., et al., 2010. Monoclonal antibody targeting of N-cadherin inhibits prostate cancer growth, metastasis and castration resistance. *Nat. Med.* 16, 1414–1420.
- Tanner, T.M., Denayer, S., Geverts, B., Van Tilborgh, N., Kerkhofs, S., Helsen, C., Spans, L., Dubois, V., Houtsmuller, A.B., Claessens, F., Haelens, A., 2010. A 629RKLKK633 motif in the hinge region controls the androgen receptor at multiple levels. *Cell. Mol. Life Sci.* 67, 1919–1927.
- Thadani-Mulero, M., Portella, L., Sun, S., Sung, M., Matov, A., Vessella, R.L., Corey, E., Nanus, D.M., Plymate, S.R., Giannakakou, P., 2014. Androgen receptor splice variants determine taxane sensitivity in prostate cancer. *Cancer Res.* 74, 2270–2282.
- Visakorpi, T., Hyytinen, E., Koivisto, P., Tanner, M., Keinänen, R., Palmberg, C., Palotie, A., Tammela, T., Isola, J., Kallioniemi, O.-P., 1995. In vivo amplification of the androgen receptor gene and progression of human prostate cancer. *Nat. Genet.* 9, 401–406.
- Vrignaud, P., Semiond, D., Lejeune, P., Bouchard, H., Galvet, L., Combeau, C., Riou, J.-F., Commercon, A., Lavelle, F., Bissery, M.-C., 2013. Preclinical antitumor activity of cabazitaxel, a semisynthetic taxane active in taxane-resistant tumors. *Clin. Cancer Res.* 19, 2973–2983.
- Yang, J., Weinberg, R.A., 2008. Epithelial-mesenchymal transition: at the crossroads of development and tumor metastasis. *Dev. Cell* 14, 818–829.
- Yilmaz, M., Christophori, G., 2009. EMT, the cytoskeleton, and cancer cell invasion. *Cancer Metastasis Rev.* 28, 15–33.
- Zhang, X., Morrissey, C., Sun, S., Ketchandji, M., Nelson, P.S., True, L.D., Vakar-Lopez, F., Vessella, R.L., Plymate, S.R., 2011. Androgen receptor variants occur frequently in castration-resistant prostate cancer metastases. *PLoS One* 6, e27970.
- Zhu, M.-L., Horbinski, C., Garzotto, M., Qian, D.Z., Beer, T.M., Kyprianou, N., 2010. Tubulin-targeting chemotherapy impairs androgen receptor activity in prostate cancer. *Cancer Res.* 70, 7992–8002.
- Zhu, M., Kyprianou, N., 2010. Role of androgens and the androgen receptor in epithelial-mesenchymal transition and invasion of prostate cancer cells. *FASEB J.* 24, 769–777.